



Memo 149

Increased SKA-Low Science Capability through Extended Frequency Coverage

D. C. Price
D. Sinclair
J. Hickish
M.E. Jones

September 2013

INCREASED SKA-LOW SCIENCE CAPABILITY THROUGH EXTENDED FREQUENCY COVERAGE

SKA MEMORANDUM 149

D. C. Price^{1,E}, D. Sinclair¹, J. Hickish¹, M.E. Jones¹

¹ University of Oxford, Keble Rd, Oxford, United Kingdom OX4 1AH

^E Author email: danny.price@astro.ox.ac.uk

In the recently published baseline design, the SKA-low telescope operates over 50 to 350 MHz. In this memo, we present performance analyses of two scenarios in which the baseline SKA-low design is augmented: by increasing the frequency performance of the SKA-low antennas; and, by splitting SKA-low into a two discrete arrays (a ‘dual-band’ implementation). We find that in either scenario, there is significant merit in extending the operational frequency range. In addition, in the case of a dual-band implementation, we find very significant (orders of magnitude) performance increase for surveys of point sources and extended emission over the current SKA-low baseline design.

1 INTRODUCTION

In the recently published SKA Baseline Design (BD, Dewdney, 2013), the SKA-low telescope has been specified to operate over a 7:1 bandwidth from 50-350 MHz. There has been discussion within the SKA community of increasing this frequency range, in order to maximize science output. However, any modification would have to significantly increase science output while still fitting in to SKA-low’s cost envelope.

In order to investigate the science capability of an extended array, one must first evaluate its performance with suitable figures of merit (FoM). In this memo, we present performance FoMs for two implementations of SKA-low with extended frequency ranges. In the first, the operational frequency range of the SKA-low antenna and low noise amplifier (LNA) are extended. We refer to this as the ‘single-band’ implementation. We secondly consider a ‘dual-band’ implementation, where the frequency range 50-190 MHz is covered with one array, and 190-650 MHz is covered with a second. These implementations are detailed further in Section 2 below.

After defining the specifications of the two representative arrays, we then examine their performance. This is done using FoMs such as system equivalent flux density and point-source survey speed. We also introduce a new FoM which is more suitable for surveys of extended sources, such as the large scale structure associated with the Epoch of Reionization. We find that there is significant merit in extending the operational frequency range of SKA-low, and that its performance is in some aspects comparable to the lowest band of the SKA-mid dish array. We also find that a dual-band implementation could conduct a point source survey as much as 9 times faster than a single-band implementation at the upper end of the SKA-low frequency range; and further, that a dual-band implementation could survey extended sources as much as 81 times faster.

2 SINGLE AND DUAL-BAND REPRESENTATIVE IMPLEMENTATIONS

There are two main ways in which the frequency coverage of SKA-low can be increased; these are shown in the cartoons of Figure 1. The first is by extending the frequency coverage of the antenna and LNA: it is feasible that a single log-periodic antenna could cover a frequency range from 50-650 MHz, and similarly a wide-bandwidth LNA could be developed. These changes would be unlikely to dramatically affect the cost of the analogue systems. So that the cost of digital systems is not increased,

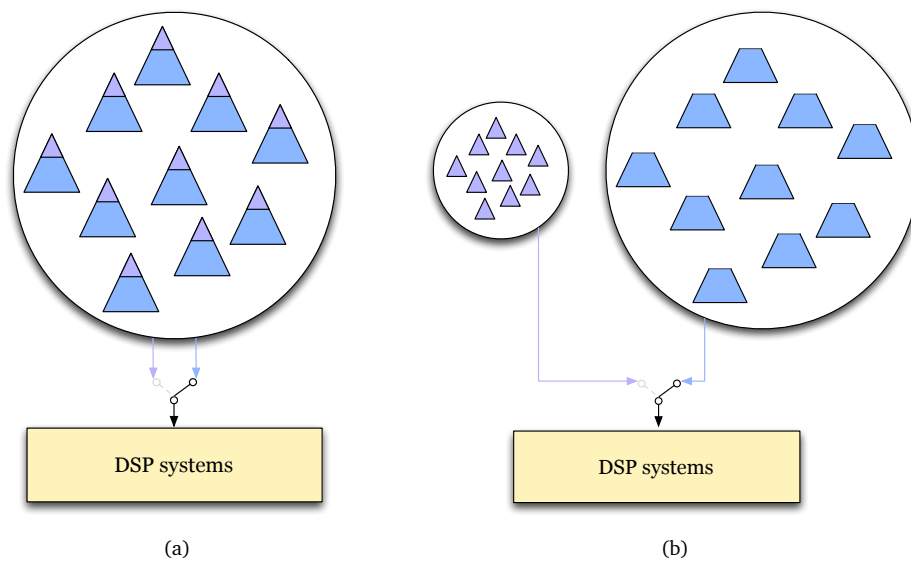


Figure 1: Cartoon diagram showing two different implementations for a frequency extended SKA-low station. Antennas are shown as shaded triangles, and the station is shown as a circle. On the left, frequency range is extended by increasing the frequency coverage of the antenna and LNA. This is shown by the purple shaded addition. On the right hand side, an entirely new array is produced, where the upper-band array is a physically scaled version of the lower-band array. Both implementations have shared DSP systems.

a selectable pair of bandpass filters over 0-350 MHz and 350-700 MHz before digitization would allow the same digital hardware to be used. The upper frequency range would hence be sampled using the second Nyquist zone of digitizers sampling at 700 MHz. The end-user would then select whether to observe the upper or lower frequency band.

A second way in which SKA-low’s frequency coverage could be extended is by building two arrays, one of which is a frequency-scaled version of the other. For example, one could implement SKA-low as two discrete arrays with $\sim 3.5 : 1$ bandwidths, with one array operating at 50-190 MHz, and another operating at 190-650 MHz. Although one might expect that such a dual-band implementation could be as much as twice as expensive, detailed cost modeling by Colegate et al. (2012) suggests that the overall cost of a dual-band implementation would be less than 50% more than the single-band alternative. Again, backend DSP could be shared between the two arrays.

Our representative SKA-low implementations are shown in Table 1, and specifications common to these implementations are given in Table 2. Note that our dual-band representative system differs to that of Colegate et al. (2012), to incorporate the recent BD specifications. As the EoR science case has been weighted heavily in the new baseline specification, in our representative dual-band implementation we will split the array at 190 MHz. This results in an array covering 50-190 MHz (‘dual-low’) and another covering 190-650 MHz (‘dual-mid’).

2.1 SCIENCE MOTIVATION

The proposed increase of the upper frequency of SKA-low is motivated by science. In the memorandum by Huynh et al. (2012), the the authors address the question:

“Assuming a frequency dynamic range of 3.5:1. in order to maximize the science return of the SKA Phase 1, is there an optimum centre frequency within the 70-450 MHz (goal: 50-450 MHz) band?”

Table 1: Representative SKA-low implementations, as used in this memorandum.

Specification		single	dual-low	dual-mid	
Frequency range		50-350	50-190	190-350	MHz
Average inter-element spacing	D_{el}	2.06	2.06	0.69	m
	($\lambda/2$ spaced at)	137	137	411	MHz
Station diameter	D_{st}	35	35	11.7	m

Table 2: Shared specifications for the representative SKA-low single and dual-band implementations.

Specification	symbol	value	
Receiver temperature	T_{rec}	$40 + 0.1T_{sky}$	K
Sky temperature	T_{sky}	$60\lambda^{2.55}$	K
System temperature	T_{sys}	$T_{rec} + T_{sky}$	K
Number of polarizations	n_p	2	
Number of beams	n_B	1	
Antenna element gain	G_A	8.0	dBi
Elements per station	N_{el}	289	
Number of stations (core)	N_{st}	650	
Number of stations (total)	N_{st}	911	

This question is particularly apt in the context of the single versus dual discussion¹; Table 3 summarizes their conclusions on optimal frequency ranges for the SKA-low science cases. From inspection of Table 3, one immediately notices that there is no 3.5:1 single-band implementation which will satisfy all the science requirements. It does, however, seem that the science goals can be divided into two partitions: low-low-frequency (54-240 MHz), and mid-low-frequency (130-450 MHz).

While Huynh et al. (2012) do not directly consider science in the frequencies range 450-650 MHz, their discussion provides support for this extended range. For example, galaxy continuum surveys with SKA-low (case 6 in Table 3) will be confusion limited; as such, a higher frequency range is preferred. Magnetism and polarization science (case 7) is also more rewarding at higher frequencies as Faraday depolarization is proportional to the wavelength squared. A high-sensitivity array at frequencies around 400 MHz is ideal for conducting a fast survey for millisecond pulsars off the Galactic plane (Roy Smits et al., 2008 and SKA Memo in prep).

An newly suggested and compelling motivation that is not currently part of the SKA key science projects is placing stringent bounds on different cosmological inflation models. In Camera et al. (2013), it is suggested that a 21-cm intensity mapping experiment (i.e. unresolved maps of HI-line emission) at $z \simeq 1 - 5$ may be used to detect the large-scale effects of primordial non-Gaussianity, giving insight into the conditions of the early Universe. A frequency extended version of SKA-low would be an ideal instrument with which to conduct a high-redshift 21-cm intensity mapping experiment.

3 PERFORMANCE METRICS FOR SKA-LOW

Many of the science goals of the SKA-low instrument require it to be able to survey large portions of the sky. If we are to compare the performance of different aperture array implementations, we must first define a set of figures of merit (FoM). Here, we consider several different FoMs with which to compare array performance. Briefly, these are:

- **System equivalent flux density (SEFD):** for targeted observations of small fields. A fundamental performance metric, but not directly applicable to key science goals.

¹this was, however, originally raised in the context of wide-bandwidth antenna performance.

Table 3: Optimal frequency ranges for SKA-low, assuming a 3.5:1 bandwidth limit. Table reproduced from Huynh et al. (2012)

ID	Science	Freq Range	Central Freq
1	EoR	54-190	101
2	21cm Forest	70-240	
3	Astrobiology	70-240	70
4	HI Absorption	130-450	
5	Gravity & Pulsars	130-450	450
6	Galaxy continuum	130-450	450
7	Magnetism	130-450	450
8	Transients		N/A

- **Point source survey speed (PFoM):** for surveys of point-source like objects, such as unresolved continuum sources. For science cases 2, 3, 4, 6 and 7 in Table 3.
- **Extended source survey speed (BFoM):** for surveys of extended sources and large scale structure, such as the epoch of reionization (EoR) signal. For science case 1, and intensity mapping experiments.

We introduce these quantities in more detail below; Section 4 then uses these to compare the performance of the representative single and dual-band implementations.

3.1 SYSTEM EQUIVALENT FLUX DENSITY

The overall sensitivity of a radio telescope is given by its flux collecting ability, coupled with its system temperature. A common figure of merit is the system equivalent flux density, SEFD:

$$\text{SEFD} = \frac{2T_{\text{sys}}k_B}{A_e}. \quad (1)$$

Here, and A_e is the effective collecting area of the telescope. The SEFD is measured in Janskys (Jy), where $1 \text{ Jy} = 10^{-26} \text{ Wm}^{-2}\text{Hz}$. An alternative metric which is also commonly used is $A/T_{\text{sys}} \propto 1/\text{SEFD}$. A large A/T_{sys} corresponds to better performance; see Thompson et al. (2004) for a more in-depth discussion.

SEFD is a useful quantity as when combined with the radiometer equation, the smallest detectable signal ΔS is given by:

$$\Delta S = m \frac{\text{SEFD}}{\sqrt{2n_p N_{st} \Delta\nu \tau}}. \quad (2)$$

Where $\Delta\nu$ is bandwidth, τ is integration time, n_p is the number of polarizations, m is a signal-to-noise threshold, and N_{st} is the number of stations within the interferometer.

3.2 POINT SOURCE SURVEY SPEED

When designing a telescope for surveys, an important metric is the survey speed. This section defines a FoM which can be used to compare the point source survey speed (PFoM) of different implementations.

As given by Equation 2, the time taken to reach a desired flux sensitivity (in Jy) for a given pointing is

$$\tau = \frac{m^2 \text{SEFD}^2}{2n_p \Delta\nu \Delta S^2}. \quad (3)$$

To survey a field of solid angle Ω_{survey} requires P pointings, where

$$P = \frac{\Omega_{survey}}{\Omega_{FoV}}. \quad (4)$$

Here, Ω_{FoV} is the instantaneous field of view (FoV) of the instrument. The total time taken is then

$$\tau P = \frac{m^2 \text{SEFD}^2}{2n_p \Delta \nu \Delta S^2} \frac{\Omega_{survey}}{\Omega_{FoV}}. \quad (5)$$

If we rearrange this so that parameters intrinsic to the instrument are equated to survey parameters, and write $\tau P = t$ as the total survey time, we find

$$\frac{\Omega_{survey} m^2}{t \Delta S^2} = \frac{2n_p \Delta \nu \Omega_{FoV}}{\text{SEFD}^2} \triangleq \text{PFoM}. \quad (6)$$

where the right hand side is defined to be the point source survey speed figure of merit (PFoM). The PFoM may be rewritten as

$$\text{PFoM} = \frac{n_p \Delta \nu \Omega_{FoV}}{2k_B^2} \left(\frac{A_e}{T_{sys}} \right)^2. \quad (7)$$

As Equation 6 relates survey parameters to an instrument's PFoM, one can use the PFoM to find the required survey time t to reach a desired sensitivity ΔS over a patch of sky Ω_{survey} . This FoM is similar to that presented in Cordes (2009); however, it differs in its inclusion of fundamental constants. The PFoM, while only approximate, is a convenient way of comparing telescope survey speed; large PFoMs correspond to instruments with faster point source survey speeds.

3.3 EXTENDED SOURCE SURVEY SPEED

Although PFoM is a useful metric for comparing point source sensitivity, to detect large scale structure (such as the EoR signal), an instrument must instead be sensitive to large scale brightness temperature fluctuations. For a fully filled aperture telescope, if the source of interest does not fill the beam, then the minimum temperature detectable is

$$\Delta T = \frac{m T_{sys}}{\sqrt{2n_p \Delta \nu \tau}} \frac{\Omega_B}{\Omega_S}, \quad (8)$$

where Ω_S is the solid angle subtended by the source.

For a sparse aperture, the (u, v) plane is not fully sampled. As such, their sensitivity to the sky brightness T_b is smaller by a 'filling' factor²

$$f = \frac{A_e}{A_{phys}}, \quad (9)$$

where A_e is the total collecting area of the array, and A_{phys} is the physical extent of the array. The brightness temperature sensitivity is then

$$\Delta T = \frac{m T_{sys}}{\sqrt{2n_p \Delta \nu \tau}} \frac{\Omega_B}{\Omega_S} \frac{1}{f}. \quad (10)$$

From Equation 10, we may derive a a brightness figure of merit (BFoM) in a similar fashion to the PFoM. Assuming our instrument has sufficient resolution such that the extended source does indeed

²This is an approximation, which assumes a minimally redundant array.

fill the beam (so $\Omega_B = \Omega_s$), we have

$$\tau P = \frac{m^2 T_{sys}^2}{\Delta T^2 2n_p \Delta v} \frac{1}{f^2}, \quad (11)$$

and the BFoM is then defined as

$$\frac{\Omega_{survey} m^2}{t \Delta T^2} = 2n_p \Delta v \Omega_{FoV} \left(\frac{f}{T_{sys}} \right)^2 \triangleq \text{BFoM} \quad (12)$$

Accordingly, the brightness temperature survey speed of a sparse aperture instrument decreases as f^2 with the filling factor. Comparing Equation 7 with Equation 12, we note that:

- Increasing the collecting area A_e while keeping f constant will increase the PFoM, but will not increase the BFoM.
- Increasing the filling factor f while keeping the collecting area A_e constant (by packing elements tighter) will increase the BFoM, but not the PFoM (so long as the source remains resolved).

This is a key point for designing an instrument sensitive to large scale structure such as the EoR signal. In the section that follows, we apply these FoMs to evaluate the performance of SKA-low implementations.

4 RESULTS

With the set of FoMs introduced above, we are now well equipped to compare the various FoMs of the single and dual-band stations. The proposed frequency extension of SKA-low creates an overlap between the upper frequency range of SKA-low and the lower frequency range of the SKA-mid dish array (band 1). Various figures of merit are shown as a function of frequency in Figure 2, for the single and dual-band implementations summarized in Table 1 and Table 2. Also plotted are the FoMs for the SKA-mid band 1 dish array, using the specifications from the BD.

SEFD AND A/T In Figure 2a, the SEFD for the single and dual-band implementations³ are shown as a function of frequency; Figure 2b. shows the A/T_{sys} . When both the dual-mid and single-band implementations are in their sparse regime, their SEFDs are equal. However, when the dual-mid array is in its dense regime, its collecting area is limited to πr^2 , and as such its SEFD and A/T_{sys} are retarded.

POINT SOURCE FoM While the SEFD of an aperture array is fixed by the collecting area and system temperature, survey speed FoMs are a function of the field of view (Figure 2c). As such, we need to take into account the number of beams and the field of view of each beam (in the current baseline specification, each aperture array has a single beam).

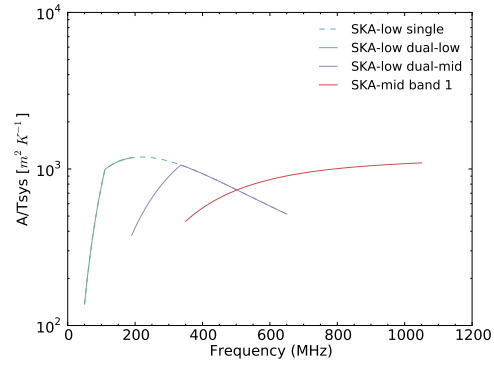
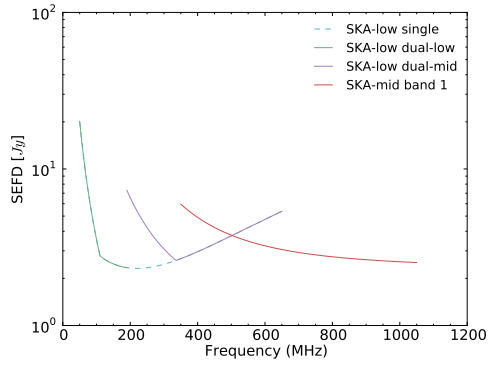
For a single-band implementation, the PFoM for a single aperture array station is given by Equation 7:

$$\text{PFoM}_{single} = \frac{n_p n_B \Delta v \Omega_B}{2k_B^2} \left(\frac{A_e}{T_{sys}} \right)^2, \quad (13)$$

with $\Omega_{FoV} = n_B \Omega_B$, where n_B is the number of beams and Ω_B is the solid angle of a single beam, which is defined as

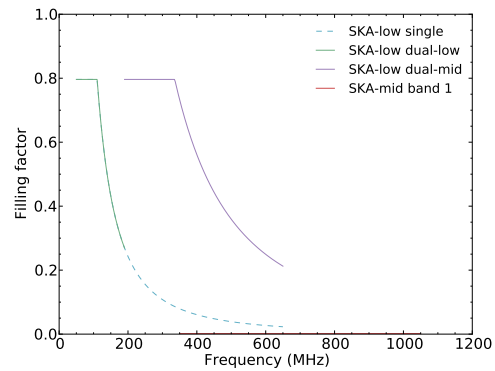
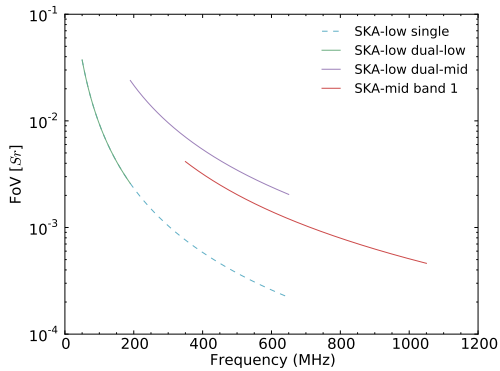
$$\Omega_B = \frac{\lambda^2}{A_e}. \quad (14)$$

³We assume that the station is phased to zenith; when a beam is pointed away from zenith, the effective area decreases due to projection effects; this is not considered.



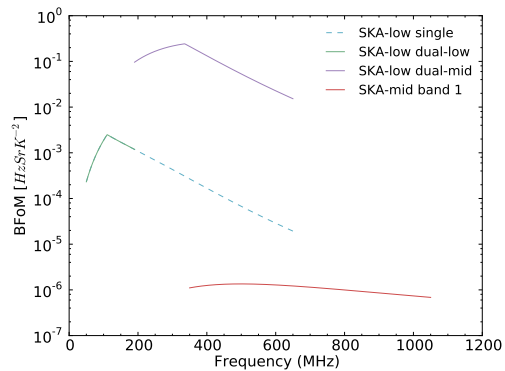
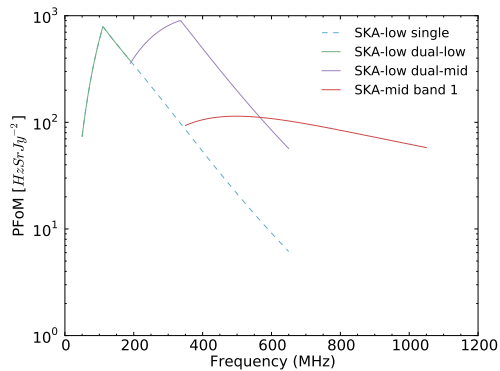
(a) SEFD for the single and dual-band SKA-low representative implementations, as a function of frequency.

(b) A/T_{sys} (proportional to $1/\text{SEFD}$), for the single and dual-band SKA-low representative implementations, as a function of frequency.



(c) Field of view (FoV) for the single and dual-band SKA-low representative implementations, as a function of frequency.

(d) Filling factor of the core region for the single and dual-band SKA-low representative implementations, as a function of frequency.



(e) Point source survey speed (PFoM) for representative SKA-low implementations. The increase field of view of the dual-mid array boosts its PFoM in comparison to the single-band implementation.

(f) Brightness sensitivity survey speed (BFoM) for representative SKA-low implementations. The larger field of view of the dual-mid array, coupled with an increased filling factor, makes its BFoM significantly higher than the single-band implementation.

Figure 2: Performance characteristics of the SKA-low representative arrays. While the A/T_{sys} of the dual-mid implementation is lower than that of the single-band, its increased field of view (per beam) significantly boosts its PFoM and BFoM.

The system temperature of the array can be expressed as the sum of receiver and sky temperatures $T_{sys} = T_{rec} + T_{sky}$.

As shown in Figure 2e, the PFoM of both the single and dual-band implementations are within an order of magnitude of that of SKA-mid band 1, with the dual-band implementation surpassing SKA-mid's performance over the lower half of band 1. The increased PFoM of the dual-band array over the single-band can be explained by its increased field of view. As given in Table 1 above, the inter-element spacing of a dual-mid station is an average 0.69 m, as compared to the single-band station at 2.05 m. It follows that when both arrays are in their sparse regime, the ratio of the single-band PFoM to that of the dual-mid array is

$$\frac{\text{PFoM}_{dual-mid}}{\text{PFoM}_{single}} = \frac{\Omega_{dual}}{\Omega_{single}} = \frac{\lambda^2/(\pi r_D^2)}{\lambda^2/(\pi r_S^2)} = 9. \quad (15)$$

That is, the PFoM of the dual-mid array is nine times higher than that of the single-band array at the upper end of the SKA-low band. It follows that point source surveys at dual-mid frequencies will be significantly slower with a single-band implementation than with a dual band. It should be noted that we have indeed made a trade-off: the angular resolution of each dual-mid array is three times lower than the single-band implementation, and we have retarded A/T_{sys} at the lower frequency end of the dual-mid array. Nevertheless, as we intend to operate SKA-low as an interferometric synthesis array, the overall angular resolution of SKA-low will instead depend upon inter-station baseline lengths.

EXTENDED SOURCE FoM To compare sensitivity to extended sources, we must consider the filling factor of the two arrays. The overall filling factor is given by

$$f = f_{st} f_{core}, \quad (16)$$

where f_{st} is the filling factor of the station, and

$$f_{core} = N_{st} A_{st} / \pi r_{core}^2 \quad (17)$$

is the filling factor of the core, $f_{core} \approx 0.8$. We have used a simple model where f_{st} is set to 1 if the sum of antenna collecting areas is larger than the physical area of the array, and do not consider coupling or effects due to area overlap; see Figure 2d.

The core of SKA-mid dish array is much more sparsely filled than the two SKA-low implementations. As such, its BFoM is drastically lower. This is shown in Figure 2f as a function of frequency. Over the dual-low band, we have $\text{BFoM}_{single} = \text{BFoM}_{dual-low}$. For the dual-mid array, when both arrays are in their sparse regime, the ratio of brightness sensitivities becomes

$$\frac{\text{BFoM}_{dual-mid}}{\text{BFoM}_{single}} = \frac{\Omega_{dual} f_{dual}^2}{\Omega_{single} f_{single}^2} = 9 \times 9 = 81, \quad (18)$$

i.e. at the upper end of the SKA-low band, the dual-mid array has 81 times the brightness sensitivity survey speed of the single-band implementation. Of course, the overall brightness sensitivity of SKA-low also depends upon how tightly packed the stations are: the inter-station spacing within the core must also be reduced by the same factor to maintain this 81 times improvement in BFoM.

To illustrate how drastic this difference in performance is, over a 1 month (28 day) period, with a threshold $m = 5$ the dual-mid array could reach a temperature sensitivity of $\Delta T \sim 7\text{mK}$ over a 1 steradian patch of sky. It would take over six years for the SKA single-band implementation (as considered here) to reach this level.

5 DISCUSSION

Both the single and dual-band implementations of SKA-low considered above have PFoMs comparable to the SKA-mid dish array. If the inherent multibeaming capabilities of the SKA-low aperture array were to be leveraged, they could significantly outperform the SKA-mid band 1 in surveys of point sources. However, calibration may be a limiting factor for SKA-low at the upper end of its frequency range, as the array will be very sparse. We shall not consider calibration any further here, but do stress that it must be seriously considered.

From the PFoM and BFoMs computed above, it is clear that a dual-band SKA-low will perform significantly better at the upper frequencies of SKA-low's band than a single-band implementation. But do we need this boost in performance?

If we consider only the most recent baseline design, EoR and HI-line absorption science cases have been prioritized (Dewdney, 2013), with pulsar, transient and all other science cases (Table 3) shifted into the SKA-mid. The EoR science case does not require frequency coverage at dual-mid frequencies, so we may therefore rephrase the question as: does a higher survey speed (PFoM) strengthen HI-absorption science outcomes? The answer to this is currently unclear, and will require input from the HI-absorption science consortium.

On the other hand, if we consider the more extensive science cases discussed in Huynh et al. (2012), it is more convincing that a dual-band implementation would be beneficial. Huynh et al. (2012) also suggest that higher frequency coverage would be greatly beneficial. A dual-band implementation may indeed allow this, if 3.5:1 antenna element covered the 190-650 MHz band. As EoR observations will likely be conducted only at night-time and when the galactic plane is low, it is unlikely that SKA-low will be used for EoR more than 1/3 of the year. An extended frequency range may allow higher utilization if science in the upper frequency range can be conducted during the day.

Given the significant boost in performance and potential corresponding increase in science capability, we strongly suggest that frequency extended implementations are investigated further. One factor that may limit band extension is cost: we briefly discuss this below for the dual-band implementation.

5.1 COST COMPARISON

As is shown in the tour-de-force of Colegate et al. (2012), costing SKA-low is a fiendishly hard task. To give a simple illustration here, one might expect that building two identical copies of the SKA-low single-band implementation would cost twice as much as building only one. In reality, this is unlikely to be the case due to economies of scale; for example, the cost of transporting earthmoving equipment and non-recoverable tooling expenses would be incurred once, not twice.

Nonetheless, if the cost of a dual-band implementation is close to twice that of a single band, it is probably not a viable option. We do not believe that this is the case, for the following reasons:

- In the case of a bandwidth-conserving split, the computational requirements of SKA-low do not change. As such, one would expect the cost of the correlator and beamforming systems to remain about the same.
- Antennas with narrower bandwidths are, in general, cheaper (and smaller) than wide-band antennas. For example, the top portion of a log-periodic antenna can essentially be 'lopped off' and used as an antenna in its own right.
- One could investigate a single signal processing system shared between dual-low and dual-mid, which processes only half of the current bandwidth specification (i.e. 150 MHz as opposed to 300 MHz). Decreasing the input bandwidth of the correlator would give a significant cost savings, which could counterbalance any increase in analogue costs.

- In terms of analogue cabling, the dual-mid array would require shorter lengths of cable due to its diminished size.
- If the survey speed of an instrument is increased, the required time per survey is shorter. So, total power consumption may in fact be lower for dual-band implementation, as surveys may potentially take an order of magnitude less time.
- The dual-mid array does not need to have as many elements as the dual-low to maintain higher survey speeds. The size could be decreased in order to remain within a given cost envelope.

To summarize these points: we suggest that a dual-band implementation with a shared digital signal processing system may in fact be comparable in cost to a single-band implementation.

5.2 DUAL-BAND ADVANTAGES

The main advantage of a dual-band implementation is that the survey speed is significantly boosted. We now briefly outline some additional motivations for further investigation into dual-band implementations:

- One of the large unknowns for the SKA-low project is how well the array can be calibrated when it is very sparse. A dual-band implementation would mitigate this potentially serious risk.
- Splitting the array into two would ease the requirements for low noise amplifier design, as the T_{sys} of the dual-low array would be dominated by sky noise, while the T_{sys} of the dual-mid array would be dominated by receiver noise.
- If the dual-mid array had a 3.5:1 bandwidth range, it would allow operation at up to 650 MHz. This would be advantageous for pulsar studies. The second or third nyquist zone of the digitizers could be used, along with aliasing filters, to avoid the need for downconversion.
- As star formation rate peaks at $z \sim 2$, many authors have proposed intensity mapping experiments for redshifted HI at frequencies 400-800 MHz, for example, the Canadian-led CHIME project⁴. The dual-mid array could potentially conduct an intensity mapping survey at 400-650 MHz, as it retains a high BFoM over this range. Such an experiment would place stringent bounds on different models of inflation (Camera et al., 2013).
- Huynh et al. (2012) suggest that higher frequency coverage is also advantageous for the science cases 4, 5, 6 and 7 in Table 3.
- The dish-based SKA-mid is likely to be highly oversubscribed, whereas SKA-low may be dormant for a large fraction of time. If some of the science from SKA-mid can be shifted back to SKA-low, it could potentially increase the science output of the SKA.
- If SKA-low's science-capable frequency range was extended, it may allow for SKA-mid's operational frequency requirements to be eased. This could simplify band 1 receiver development.

In summary, a dual-band implementation is less risky and potentially has far greater science capability. This should be weighed against its cost, which is likely increased over the single-band SKA-low.

⁴The Canadian Hydrogen Intensity Mapping Experiment, <http://chime.phas.ubc.ca/>

6 CONCLUSIONS

In this memo, we have contrasted the performance of single-band and dual-band implementations of SKA-low with extended frequency coverage. We have shown that the point source survey speed (PFoM) of both implementations is comparable to that of the SKA-mid dish array over the considered frequency extension. Additionally, we have shown that the dual-band significantly outperforms the single in terms of PFoM and extended source survey speed (BFoM) at the high frequency end of this extended SKA-low operational range. Further, both implementations have significantly higher BFoMs than the SKA-mid array.

Whether or not it is viable to pursue an extended frequency range SKA-low will depend upon the increase in cost versus the increase potential science output, and the calibratability of the array at the upper end of the frequency range. We argue that the cost increase would be modest, and the science capability would increase significantly. As such, we strongly suggest that more detailed cost modelling is conducted and that the science case for SKA-low is re-examined with reference to an extended frequency range.

REFERENCES

- Camera, S., Santos, M. G., Ferreira, P. G., & Ferramacho, L. (2013). Cosmology on Ultra-Large Scales with HI Intensity Mapping: Limits on Primordial non-Gaussianity. *arXiv.org*, (pp. 6928).
- Colegate, T. M., Hall, P. J., & Gunst, A. W. (2012). Memo 140: Cost-effective aperture arrays for SKA Phase 1: single or dual-band? *SKA Memo Series*.
- Cordes, J. (2009). Memo 109: Survey Metrics. *SKA Memos*, (pp. 1–6).
- Dewdney, P. (2013). SKA1 System Baseline Design. *SKA Project Documents*, (pp. 1–98).
- Huynh, M., van Bemmell, I., Koopmans, L., et al. (2012). Is There an Optimum Frequency Range for SKA1-lo? Question 1 of the Magnificent Memoranda II. *SKA Memo Series*, (pp. 1–37).
- Roy Smits, Kramer, M., Stappers, B., et al. (2008). Memo 105: Pulsar searches and timing with the SKA. *SKA Memo Series*, (pp. 1–14).
- Thompson, A. R., Moran, J. M., & Jr., G. W. S. (2004). *Interferometry and Synthesis in Radio Astronomy*. WILEY-VCH Verlag, second edition.